Chaos Synchronization Error Compensation by Neural Network

Junxiang Ke, Lilin Yi, *Member, IEEE*, and Weisheng Hu, *Member, IEEE*

***Abstract*— Chaos synchronization is the foundation of chaotic optical communications. The parameter mismatch between chaotic transmitter and receiver will significantly degrade the synchronization performance. In this letter, neural network is proposed to improve the performance of chaos synchronization. The compensation for chaos synchronization error caused by the mismatch of different hardware parameters, such as frequency response, loop gain, modulator bias, and time delay, has been discussed and analyzed in simulation and experiment. Compared with other digital signal processing (DSP) algorithms including feed-forward equalization and Volterra filter, neural network shows best performance. In some occasions, the cross correlation can be improved from 0 to 0.8. Further, the performance improvement in chaotic optical communications by neural network has been verified in simulation. This technique has potential to be used in high-speed chaotic optical communications.**

***Index Terms*— Optical communication, optical secure and encryption, chaos.**

I. Introduction

CHAOTIC communications based on chaos synchronization was first proposed in the early 1990s [1]. Since then, attributed to the potential applications in high-speed secure communications, many new schemes have been proposed to realize chaotic optical communications [2]–[8], which are mainly based on the nonlinearity of modulators and semiconductor lasers. For all chaotic optical communication schemes, the most important function is chaos synchronization. Compared with laser-based scheme, chaos synchronization in modulator-based scheme is simplified and easier for implementation [2]–[8]. In high-speed chaotic optical communications, wideband chaos generation and high quality wideband chaos synchronization are required, which increase the difficulty of implementation. Many wideband chaos generation schemes have been proposed [9], [10] but wideband chaos synchronization with high quality is still hard to realize. Therefore, from the viewpoint of practical implementation, a very stable and accurate synchronization between the emitter and receiver is very important. Adaptive synchronization of chaotic system has been proposed to improve the synchronization performance [11], [12], but the chaotic bandwidth has been limited by the electronics in the loop.

Manuscript received March 15, 2019; revised April 27, 2019; accepted May 21, 2019. Date of publication May 29, 2019; date of current version June 19, 2019. This work was supported by the National Natural Science Foundation of China under Grant 61575122. *(Corresponding author: Lilin Yi.)*

The authors are with the State Key Laboratory of Advanced Optical Communication Systems and Networks, Shanghai Institute for Advanced Communication and Data Science, Shanghai Jiao Tong University, Shanghai 200240, China (e-mail: lilinyi@sjtu.edu.cn).

Color versions of one or more of the figures in this letter are available online at http://ieeexplore.ieee.org.

Digital Object Identifier 10.1109/LPT.2019.2919804

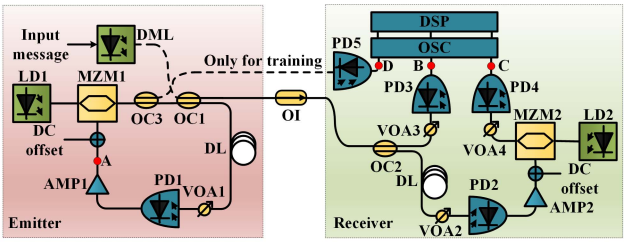

Fig. 1. Simulation and experiment setup. LD, laser diode; DML, direct-modulated laser; MZM, Mach-Zehnder modulator; VOA, variable optical attenuator; OC, optical coupler; DL, delay line; PD, photodiode; AMP, broadband radio frequency amplifier; SMF, single mode fiber; OSC, oscilloscope.

In this work, neural network (NN) filter in the chaotic receiver side is proposed to improve the performance of chaos synchronization. For the mismatch of different physical parameters including frequency response, loop gain, modulator bias and time delay in modulator-based chaotic optical systems, NN filter is used to improve the synchronization performance in both simulation and experiment. Feed-forward equalization (FFE) and Volterra filter are used for comparison. The simulation and experiment results show that NN filter has the best performance and the cross correlation can be improved from 0 to 0.8 for the case of multi-parameter mismatch. And the performance improvement in chaotic optical communications by NN has been verified in simulation.

II. Principle And Setup

The simulation and experiment setup is shown in Fig. 1. Firstly, the chaos synchronization without message has been studied, the chaotic emitter consists of a closed-loop electro-optical feedback configuration with following components: a Mach-Zehnder modulator (MZM1) with a half voltage of $V_{\pi RF1}$ injected by a continue-wave (CW) light from laser diode (LD1) with power P_1, which provides nonlinear transfer function $cos^2(x + \varphi_1)$, where φ_1 is the DC offset of MZM1. A 50:50 optical coupler (OC1) is used to split chaotic carrier for transmission and feedback. A photodiode (PD1) with sensitivity S_1 is used to convert the optical feedback signal into an electrical one. A variable optical attenuator (VOA1) is used to control the injection power of PD1, so the feedback strength can be controlled. An electronic amplifier (AMP1) with gain G_1 is used to drive the MZM1. The whole attenuation of feedback loop is η_1, and the delay time of feedback loop tuned by delay line (DL) is T_1. Let $h_1(t)$ be the impulse response of the electronic feedback in emitter, and $V_A(t)$ be the signal at point A in Fig. 1. Then the normalized variable

$x_A(t) = \pi V_A(t)/(2V_{\pi RF1})$ can be expressed as:

$$x_A(t) = \beta_1 h_1(t) * \cos^2[x_A(t - T_1) + \varphi_1], \quad (1)$$

where $[*]$ denotes the convolution operation, and $\beta_1 = \pi P_1 \eta_1 S_1 G_1/(2V_{\pi RF1})$ represents the whole feedback strength in emitter. The above equation represents the process of chaos generation. In order to simplify the model, first-order band-pass filter is used to represent the impulse response $h_1(t)$ of the electronic feedbackin simulation, which can be expressed as:

$$h_1(t) = (\frac{1}{\tau_1}e^{-t/\tau_1} - \frac{1}{\theta_1}e^{-t/\theta_1})u(t), \quad (2)$$

where τ_1 and θ_1 are the high cutoff response time and low cutoff response time of the electronic feedback. The corresponding frequencies are $\nu_{hf1} = (2\pi\tau_1)^{-1}$ and $\nu_{lf1} = (2\pi\theta_1)^{-1}$, u(t) is Heaviside step function.

In receiver side, the input light is split into two beams by 50:50 OC2. One branch is directly detected by PD3 with sensitivity S_3 after being attenuated by VOA3. Let $h_3(t)$ be the impulse response of PD3, and $V_B(t)$ be the signal at point B in Fig. 1. Then the normalized variable $x_B(t) = \pi V_B(t)/(2V_{\pi RF2})$ can be expressed as:

$$x_B(t) = S_3\eta_3 P_1 \cos^2\Big\{\beta_1 h_1(t) * \cos^2 \times [x_A(t - T_1 - T_2) + \varphi_1] + \varphi_1\Big\} * h_3(t), \quad (3)$$

In this equation, T_2 and η_3 denote delay time and attenuation for signal transmitted from point A to point B. The expression of $h_3(t)$ is similar with the Eq. 2, where τ_3 and θ_3 represent the high cutoff response time and low cutoff response time of PD3.

The other branch is used for chaos republication, which consists of an open-loop configuration with following components: a MZM2 with a half voltage of $V_{\pi RF2}$ injected by a CW light from LD2 with power P_2, which provides nonlinear transfer function $cos^2(x + \varphi_2)$, where φ_2 is the DC offset of MZM2. A PD2 with sensitivity S_2 is used to convert the optical signal into an electrical one. A VOA2 is used to control the injection power of PD2. An AMP2 with gain G_2 is used to drive the MZM2. The whole attenuation from LD1 to the output of AMP2 is η_2. The attenuation from LD2 to PD4 is η_4. Let $h_2(t)$ be the whole impulse response of the open-loop receiver, including PD2, AMP2 and MZM2, $h_4(t)$ be the impulse response of PD4 with sensitivity S_4, and $V_C(t)$ be the signal at point C in Fig. 1. Therefore, the normalized variable $x_C(t) = \pi V_C(t)/(2V_{\pi RF2})$ can be expressed as:

$$x_C(t) = S_4\eta_4 P_2 \cos^2\Big\{\beta_2 h_2(t) * \cos^2 [x_A(t - T_3) + \varphi_1] + \varphi_2\Big\} * h_4(t), \quad (4)$$

where $\beta_2 = \pi P_1 \eta_2 S_2 G_2/(2V_{\pi RF2})$ represents the whole gain of the open-loop receiver. The expressions of $h_2(t)$ and $h_4(t)$ are similar with Eq. (2), where τ_2 and θ_2 are the whole high cutoff response time and low cutoff response time of PD2, AMP2 and MZM2, τ_4 and θ_4 are the high cutoff response time and low cutoff response time of PD4.

When the chaos synchronization is perfect, $x_B(t)$ is equal to $x_C(t)$. According to Eq. (1)-Eq. (4), perfect emitter-receiver matching conditions can be expressed as:

$$\begin{cases} \tau_1 = \tau_2, \theta_1 = \theta_2, \tau_3 = \tau_4, \theta_3 = \theta_4 \\ \beta_1 = \beta_2, \varphi_1 = \varphi_2, T_1 + T_2 = T_3, S_3\eta_3 P_1 = S_4\eta_4 P_2, \end{cases} \quad (5)$$

In order to improve the performance of chaos synchronization under parameter mismatch conditions, NN filter is proposed. NN filter, FFE and Volterra filter are widely used in high-speed long-distance optical communication [13]–[15]. In simulation and experiment of chaos synchronization, the inputs of filters are the time series measured from PD4 by oscilloscope (OSC), and the desired outputs are the time series measured from PD3 by OSC. The parameters of filters are adjusted to find the best performance of chaos synchronization. At first, the performance will become better as the input taps of filters increase, then it will become stable. The maximum order number of Volterra kernel is 3, and the NN filter consists of one input layer with 71 neurons, one hidden layer with 71 neurons and one output layer with 1 neuron. And the number of neurons will be slightly tuned to get the best performance. The activation function is max(0, x).

In order to evaluate the performance of synchronization, the normalized cross correlation function C is used to measure the chaos synchronization performance between emitter and receiver, which is defined as:

$$C = \frac{\langle [x(t) - \langle x(t)\rangle][y(t) - \langle y(t)\rangle]\rangle}{\sqrt{\langle [x(t) - \langle x(t)\rangle]^2\rangle \langle [y(t) - \langle y(t)\rangle]^2\rangle}}, \quad (6)$$

where x(t) is the time trace of emitter, and y(t) is the time trace of receiver, $\langle\cdot\rangle$ denotes average.

In simulation, the parameters in emitter remain unchanged where $\tau_1 = 20ps$, $\theta_1 = 3.18ns$, $\tau_3 = 20ps$, $\theta_3 = 1.6\mu s$, $\beta_1 = 4$, $\varphi_1 = \pi/4$, $T_1 + T_2 = 30ns$, while every parameter in receiver is changed respectively. The simulation time is $16\mu s$, the sampling rate of oscilloscope is 100 GS/s, and 1 000 000 points are used to calculate cross correlation function.

In experiment, the output power of LD1 is 14 dBm, the half voltage of MZM1 and MZM2 is 3.8V, the bandwidth of MZM1 and MZM2 is 10 GHz, the sensitivity of PD1 and PD2 is 125 mV/mW, the bandwidth of PD1 and PD2 is 10 GHz, the gain of AMP1 and AMP2 is 45 dB, the bandwidth of AMP1 and AMP2 is 10 GHz, the sampling rate of oscilloscope is 80 GSa/s and the bandwidth of each channel is 30 GHz. In the experiment, the parameter in emitter is fixed, where the injection power of PD1 is fixed at 0.36 mW, the DC offset of MZM1 is fixes at 0.184V, which is corresponding to $\varphi_1 = \pi/4$. VOA2 is tuned to change the injection power of PD2 from 0.28 mW to 0.44 mW, corresponding to the different open loop gain in receiver, which simulates the mismatch between β_1 and β_2. The DC offset of MZM2 in receiver is tuned from 1.298V to 5.298V, which is corresponding to the mismatch between φ_1 and φ_2. When the DC offset of MZM2 is 3.298V, φ_2 is $\pi/4$, corresponding to the best synchronization performance. In addition, the mismatch of time delay is tuned by the channel delay of oscilloscope.

Furtherly, the performance improvement of chaotic optical communications in back to back situation by NN filter has also been studied by simulation. As shown in Fig. 1, the output light of the direct-modulated laser (DML) modulated by 5Gb/s non-return-to-zero on-off-keying (NRZ-OOK) signal is mixed with the output light of MZM1, the mixture ratio is defined as the ratio of the message amplitude to the chaos amplitude. The mixture ratio in our simulation is set at 0.95 to make sure that the chaos can completely mask the message. The PD5 which has the same parameters with PD3 is used to detect the signal extracted from the output of MZM1 by OC3 before mixture. In the training stage, the output of PD4 is filtered by NN filter for minimizing the error between the output of PD5 and PD4. Once the training process is completed, the branch including PD5 will be dis-connected, and the trained filters can be used to filter the output of PD4. The message can be recovered by the subtraction between the output of PD3 and the filtered output of PD4. However, the eavesdroppers cannot get the output of PD5 for training if they cannot physically access the transmitter, even if the eavesdroppers try to train the parameters of NN when there is no message, the parameters of NN cannot be applied to crack the system when there is message. Because the message takes part in the chaos generation, which has great influence on the nonlinearity of chaos, therefore guarantees the system security. In practical applications, the parameters of NN filter will be trained in back-to-back situation at first, then the parameters will be saved in the receiver. It was noted that the output of PD5 is different from the output of PD3, because the message takes part in the chaos generation, the output of PD3 contains the chaos and message, but the output of PD5 only contains the chaos.

III. Results And Discussion

First of all, the improvement of chaos synchronization in single-parameter and multiple-parameter mismatch conditions by NN, FFE and Volterra filter are studied through simulation. The results are shown in Fig. 2.

The mismatch between τ_1 and τ_2 is the high cutoff response time mismatch between the combined frequency response of PD1, AMP1, MZM1 in emitter and that of PD2, AMP2, MZM2 in receiver. Defining $\Delta\tau_1 = \tau_2 - \tau_1$, as shown in Fig. 2(a), all three DSP algorithms can compensate the degradation of cross correlation function caused by the mismatch of τ_1 and τ_2. However, compared with the FFE, Volterra and NN filters have better performance, because the frequency mismatch in loop will be converted to nonlinear mismatch by MZM, and nonlinear filters can compensate the nonlinear mismatch induced degradation. Then, the mismatch between low cutoff response time θ_1 and θ_2 has also been studied. Defining $\Delta\theta_1 = \theta_2 - \theta_1$, as shown in Fig. 2(b), the cross correlation is not affected by the mismatch of θ_1 and θ_2, because θ_1 corresponds to 50 MHz, and the mismatch is also the order of MHz, which barely has influence on chaos synchronization with the bandwidth of 8 GHz. The mismatch of τ_3 and τ_4 and the mismatch of θ_3 and θ_4 is linear frequency response mismatch of PD3 and PD4, which can be completely compensated by all three algorithms, which is not shown in Fig2.

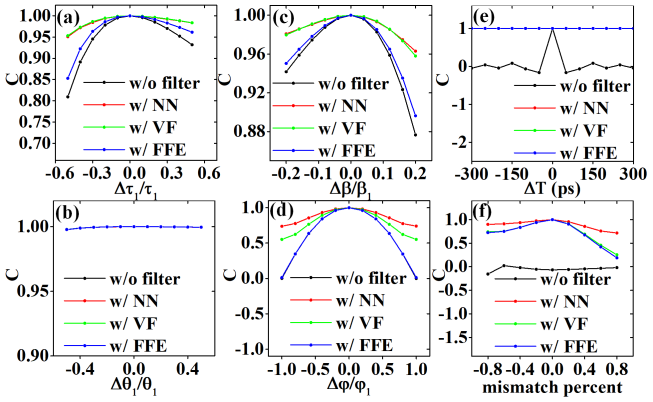

Fig. 2. The simulation results of cross correlation function C for single-parameter and multiple-parameter mismatch cases. VF, Volterra filter, (a) cross correlation function C for the mismatch between τ_1 and τ_2 with and without DSP, (b) cross correlation function C for the mismatch between θ_1 and θ_2 with and without DSP, (c) cross correlation function C for the mismatch between β_1 and β_2 with and without DSP, (d) cross correlation function C for the mismatch between φ_1 and φ_2 with and without DSP, (e) cross correlation function C for the mismatch between $T_1 + T_2$ and T_3 with and without DSP, (f) cross correlation function C for multiple-parameter mismatch with and without DSP.

The mismatch of β_1 and β_2 is then analyzed, which will affect the nonlinearity of MZM1 and MZM2, therefore, compared with linear filter, Volterra and NN nonlinear filters have better performance, as shown in Fig. 2(c), where $\Delta\beta = \beta_2 - \beta_1$. Similarly, Volterra filter and NN filter have better performance in the improvement for chaos synchronization degradation caused by the mismatch of φ_1 and φ_2, as shown in Fig. 2(d), where $\Delta\varphi = \varphi_2 - \varphi_1$, since φ corresponds to the modulator bias and will affect the nonlinearity of the modulator. The delay time mismatch is also analyzed, defining $\Delta T = T_1 + T_2 - T_3$. As shown in Fig. 2 (e), the degradation caused by delay time mismatch can be completely compensated by three algorithms since the algorithms simply act as a variable time delay when all the other parameters are matched. Finally, the multiple parameter mismatch is also studied, where the time delay mismatch is fixed at 100ps ($\Delta T = 100$ps), defining mismatch percent as $\frac{\Delta\tau_1}{\tau_1} = \frac{\Delta\theta_1}{\theta_1} = \frac{\Delta\tau_3}{\tau_3} = \frac{\Delta\theta_3}{\theta_3} = \frac{\Delta\beta}{\beta_1} = \frac{\Delta\varphi}{\varphi_1}$, and the mismatch percent is changed from -0.8 to 0.8. As shown in Fig. 2(f), all three DSP algorithms can improve the performance of chaos synchronization, and the NN filter has the best performance, which shows the powerful equalizing capability of the NN.

A comparison time series before and after the NN filter in multiple-parameter mismatch are shown in Fig. 3, where the time delay mismatch is 100ps, and the mismatch percent is 20%. The time series of PD3 and PD4 without filter are shown in Fig. 3(a), corresponding to C= −0.239, and the time series of PD3 and PD4 with NN filter are shown in Fig. 3(b), corresponding to C= 0.959.

The performance improvement in chaos synchronization by NN filter has also been verified by experiment. As shown in Fig. 4, the experimental results are quite consistent with the simulation results. In the experiment, there may exist mismatch in every single device, but the DSP algorithms can compensate the degradation of chaos synchronization caused by multiple parameter mismatch. Again, NN filter shows

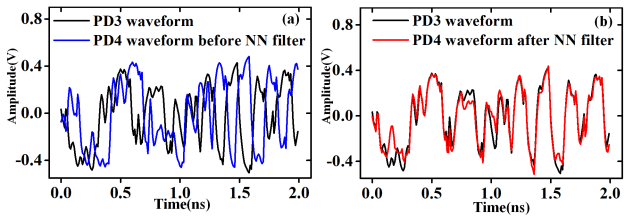

Fig. 3. Time series before and after the NN filter in multiple-parameter mismatch. (a) Time series of PD3 and PD4 before NN filter. (b) Time series of PD3 and PD4 after NN filter.

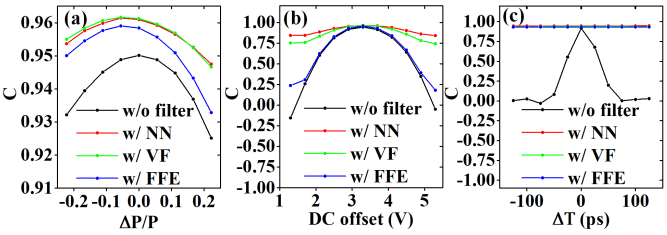

Fig. 4. The experimental results of cross correlation function C in single parameter mismatch situation. VF, Volterra filter, (a) cross correlation function C for the mismatch between the injection power of PD1 and PD2, (b) cross correlation function C for the mismatch between the DC offset of MZM1 and MZM2, (c) cross correlation function C for the mismatch of delay time.

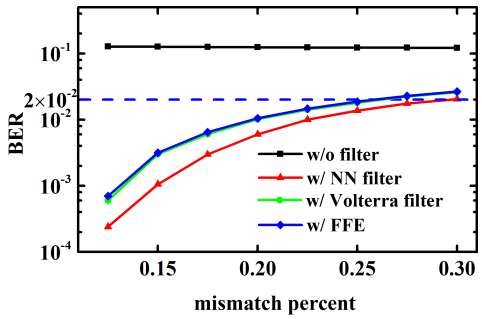

Fig. 5. The simulation results of BER for multiple-parameter mismatch situation; the dashed blue line represents the SD-FEC threshold.

powerful equalizing capability in error compensation of chaos synchronization.

Furtherly, the relationship between the bit-rate error (BER) and the parameter mismatch percent is shown in Fig. 5. The BER increases as the mismatch percent increases, and the Volterra filter has the similar performance with the FFE, but the NN filter has better performance. When BER is below than the soft decision forward error decision (SD-FEC) threshold 2e-2, the message can be effectively extracted. In this scheme, message takes part in the chaos generation, which may have influence on the performance of filter, so the performance of filter for BER in Fig. 5 is different from the performance of filter for correlation coefficient in Fig. 2(f), and when the mismatch percent is larger than 0.3, all three DSP algorithms cannot decrypt the message.

IV. Conclusion

In conclusion, thanks to NN filter, the performance of chaos synchronization can be improved. Compared with FFE and Volterra filter, NN filter has the best performance, and NN filter can be used to compensate the mismatch of all linear and nonlinear parameters, which has been verified both in simulation and experiment. Furtherly, the performance improvement of chaotic optical communication by NN filter has also been verified in simulation. We hope this technique can solve the problem of wideband chaos synchronization, which can pave the way for high-speed chaotic optical communications. Not only in chaotic optical communications, but also in other applications based on chaos synchronization, this technique provides a method to improve the performance of chaos synchronization.

References

[1] L. M. Pecora and T. L. Carroll, "Synchronization in chaotic systems," *Phys. Rev. Lett.*, vol. 64, no. 8, pp. 821–824, Feb. 1990.

[2] J.-P. Goedgebuer, P. Levy, L. Larger, C.-C. Chen, and W. T. Rhodes, "Optical communication with synchronized hyperchaos generated electrooptically," *IEEE J. Quantum Electron.*, vol. 38, no. 9, pp. 1178–1183, Sep. 2002.

[3] A. Argyris *et al.*, "Chaos-based communications at high bit rates using commercial fibre-optic links," *Nature*, vol. 438, pp. 343–346, Nov. 2005.

[4] R. Lavrov, M. Peil, M. Jacquot, L. Larger, V. Udaltsov, and J. Dudley, "Electro-optic delay oscillator with nonlocal nonlinearity: Optical phase dynamics, chaos, and synchronization," *Phys. Rev. E, Stat. Phys. Plasmas Fluids Relat. Interdiscip. Top.*, vol. 80, no. 2, Aug. 2009, Art. no. 026207.

[5] R. Lavrov, M. Jacquot, and L. Larger, "Nonlocal nonlinear electro-optic phase dynamics demonstrating 10 Gb/s chaos communication," *IEEE J. Quantum Electron.*, vol. 46, no. 10, pp. 1430–1435, Oct. 2010.

[6] J. Ai, L. Wang, and J. Wang, "Secure communications of CAP-4 and OOK signals over MMF based on electro-optic chaos," *Opt. Lett.*, vol. 42, no. 18, pp. 3662–3665, 2017.

[7] J. Oden, R. Lavrov, Y. K. Chembo, and L. Larger, "Multi-Gbit/s optical phase chaos communications using a time-delayed optoelectronic oscillator with a three-wave interferometer nonlinearity," *Chaos*, vol. 27, no. 11, Oct. 2017, Art. no. 114311.

[8] J. Ke, L. Yi, G. Xia, and W. Hu, "Chaotic optical communications over 100-km fiber transmission at 30-Gb/s bit rate," *Opt. Lett.*, vol. 43, no. 6, pp. 1323–1326, 2018.

[9] N. Jiang, C. Wang, C. Xue, G. Li, S. Lin, and K. Qiu, "Generation of flat wideband chaos with suppressed time delay signature by using optical time lens," *Opt. Express*, vol. 25, no. 13, pp. 14359–14367, 2017.

[10] A. Wang, Y. Yang, B. Wang, B. Zhang, L. Li, and Y. Wang, "Generation of wideband chaos with suppressed time-delay signature by delayed self-interference," *Opt. Express*, vol. 21, no. 7, pp. 8701–8710, 2013.

[11] B. Ravoori *et al.*, "Adaptive synchronization of coupled chaotic oscillators," *Phys. Rev. E, Stat. Phys. Plasmas Fluids Relat. Interdiscip. Top.*, vol. 80, no. 5, Nov. 2009, Art. no. 056205.

[12] T.-L. Liao and S.-H. Tsai, "Adaptive synchronization of chaotic systems and its application to secure communications," *Chaos, Solitons Fractals*, vol. 11, no. 9, pp. 1387–1396, Jul. 1999.

[13] L. Shu *et al.*, "Single-photodiode 112-Gbit/s 16-QAM transmission over 960-km SSMF enabled by Kramers-Kronig detection and sparse I/Q Volterra filter," *Opt. Express*, vol. 26, no. 19, pp. 24564–24576, 2018.

[14] Z. Li *et al.*, "Investigation on the equalization techniques for 10G-class optics enabled 25G-EPON," *Opt. Express*, vol. 25, no. 14, pp. 16228–16234, 2017.

[15] C. Ye, D. Zhang, X. Huang, H. Feng, and K. Zhang, "Demonstration of 50Gbps IM/DD PAM4 PON over 10GHz class optics using neural network based nonlinear equalization," in *Proc. Eur. Conf. Opt. Commun.*, Sep. 2017, pp. 1–3.